

# Model for retention and efficiency in open-tubular supercritical fluid chromatography

Donald P. Poe

*Department of Chemistry, University of Minnesota, Duluth, MN 55812 (USA)*

(First received May 17th, 1992; revised manuscript received July 16th, 1992)

---

## ABSTRACT

A model for open-tubular supercritical fluid chromatography at constant mass flow-rate, which takes into account the effects of temperature, density and pressure drop on solute retention and dispersion, is developed and applied to the elution of normal alkanes ( $C_8$ – $C_{40}$ ) on a polysiloxane stationary phase using  $CO_2$  mobile phase at 40 to 120°C. An exact expression for resolution is derived in terms of observed chromatographic parameters, and the effect of swelling on solute diffusion coefficients in the stationary phase is considered. Plots of apparent plate height vs. temporal average velocity show the onset of gradient-induced band spreading for a variety of conditions. Swelling of the stationary phase is shown to be critical to the achievement of acceptable efficiency for heavy solutes at low temperatures, and the prediction of a second maximum in resolution at high mobile phase velocities suggests the possibility of extremely fast separations by supercritical fluid chromatography.

---

## INTRODUCTION

The complex dependence of retention and dispersion processes in supercritical fluid chromatography (SFC) on temperature, pressure and pressure drop has been the subject of a number of investigations dealing with both packed [1–7] and open-tubular [8,9] columns. It is generally acknowledged that large pressure drops in SFC, especially near the critical point of the mobile phase, may lead to variations in retention and to a loss of efficiency beyond that which is predicted by the simple Van Deemter or Golay equations. Recent advances in chromatographic theory provide explanations for these phenomena. A unified molecular theory of chromatographic retention developed by Martire and Boehm [10,11] has provided a firm theoretical basis for the dependence of retention on temperature and mobile phase density in SFC. Further work by Martire and co-workers [12–14] developed the use of

appropriate temporal and spatial column parameters in chromatography, with one specific result being that the observed capacity factor is the temporal average value. Recently, Poe and Martire [15] provided a theoretical basis for the effect of pressure drop on efficiency in gas, liquid and supercritical fluid chromatography. The theory, which is an extension of Giddings' theory for the effect of pressure drop in gas chromatography [16], was applied to retention and band spreading for several solutes in packed column SFC, and the prediction from the theory agreed well with experimental observations. More recently Janssen *et al.* [17], using a similar approach, obtained reasonably good agreement between theory and experiment for both packed and open-tubular columns. Of particular relevance to the present investigation is that they obtained well-shaped peaks for elution of *n*-alkanes from an open-tubular column at very high velocities and large pressure drops. A general treatment of the variance of a zone in a non-uniform medium was recently published [18].

The purpose of the present study is to extend the

---

*Correspondence to:* Dr. D. P. Poe, Department of Chemistry, University of Minnesota, Duluth, MN 55812, USA.

earlier treatment of the theory for apparent plate height to provide a model for retention and efficiency in open-tubular SFC over a wide range of operating conditions, and especially to examine the effects of pressure drop and stationary phase swelling of efficiency. The column dimensions selected for application of the model represent a typical modern-day system, and in some cases the linear velocities required to generate large pressure drops are much greater than would normally be encountered in a typical laboratory setting. It is hoped that the data generated by the model will provide a basis for further experimental verification of the theory for apparent plate height, and will provide insight into open-tubular column design and operation for SFC.

## THEORY

The relevant theories for retention and efficiency in SFC are provided elsewhere [10,12,13,15]. Some of the major arguments are presented here for clarity with specific emphasis on open-tubular columns, and an exact equation for resolution is developed. In the treatment that follows, the following assumptions are made.

(1) Mass flow-rate is constant. Density programming is not considered.

(2) The column is a uniform tube, and except for the effect of mobile phase density on film thickness, it is coated with a uniform film of stationary phase.

(3) Temperature is constant, and the column and mobile phase are at thermal equilibrium. Temperature gradients due to expansion of the mobile phase and viscous flow are assumed to be negligible.

(4) Laminar flow is maintained. In the model, the Reynolds number is not allowed to exceed 1400.

### Retention

The dependence of capacity factor on temperature and density in SFC was expressed in general form by Martire and Boehm [10] as

$$\ln k' = \ln k'^0 + \Delta + a\rho_R - b\rho_R/T_R + c\rho_R^2/T_R \quad (1)$$

where  $k'^0$  is the ideal gas chromatography (GC) capacity factor,  $T_R$  and  $\rho_R$  are reduced temperature and density of the mobile phase,  $a$ ,  $b$  and  $c$  depend on solute and mobile phase properties, and  $\Delta$  accounts for sorption of mobile phase by the stationary phase.

The apparent capacity factor, which is the value observed at the column outlet, has been shown to be the temporal average of the local value [12,14]

$$\hat{k}' = \langle k' \rangle_t \quad (2)$$

Details for calculating  $\langle k' \rangle_t$  and other average quantities are given in ref. 13.

### Efficiency

For an open-tubular column under conditions of laminar flow the Golay equation describes the solute dispersion exactly.

$$H = \frac{2D_m}{u} + \frac{ud_c^2(1 + 6k' + 11k'^2)}{96D_m(1 + k')^2} + \frac{2ud_f^2k'}{3D_s(1 + k')^2} \quad (3)$$

where  $H$  is plate height,  $D_m$  and  $D_s$  are diffusion coefficients in the mobile and stationary phases,  $u$  is linear velocity of the mobile phase,  $d_c$  is column diameter, and  $d_f$  is the stationary phase film thickness.

In a previous paper [15] it was shown that the variation of  $k'$  and  $\rho$  along the axis of the column generates solute velocity gradients, which in turn give rise to gradient-induced band spreading (GIBS). For a column of uniform geometry operated under isothermal, steady-state conditions, the apparent plate height observed at the outlet of the column was shown to be

$$\hat{H} = \frac{\langle H(1 + k')^2 \rho^2 \rangle_z}{\langle (1 + k') \rho \rangle_z^2} \quad (4)$$

or the equivalent expression

$$\hat{H} = \frac{\langle H(1 + k')^2 \rho \rangle_t}{\langle 1 + k' \rangle_t^2 \langle \rho \rangle_z} \quad (5)$$

where the subscripts  $z$  and  $t$  indicate the spatial and temporal averages of the quantities in brackets.

In open-tubular SFC the internal diameter of the column may vary due to swelling of the stationary phase, resulting in variations in the column permeability and specific mass flow-rate ( $F$ , the mass flow-rate per unit area). It may be shown that for this case the exact expression for apparent plate height is

$$\hat{H} = \frac{\langle H(1 + k')^2 \rho^2 / F^2 \rangle_z}{\langle (1 + k') \rho / F \rangle_z^2} \quad (6)$$

If the variation in column diameter is on the order of a few percent or less, as it appears to be in open-tubular SFC with a typical phase ratio of 50 (see below), this variation will produce no significant effect on the apparent plate height, and eqn. 4 or 5 may be used.

Application of eqn. 5 to the Golay equation yields the desired expression for apparent plate height in open-tubular SFC,

$$\hat{H} = \frac{1}{\langle 1 + k' \rangle_i^2 \langle \rho \rangle_z} \left[ 2 \langle D_m \rho (1 + k')^2 / u \rangle_t + \frac{1}{96} \langle u d_c^2 (1 + 6k' + 11k'^2) \rho / D_m \rangle_t + \frac{2}{3} \langle u d_f^2 k' \rho / D_s \rangle_t \right] \quad (7)$$

The corresponding expression for the apparent reduced plate height is

$$\hat{h} = \frac{1}{\langle 1 + k' \rangle_i^2 \langle \rho \rangle_z} \left[ 2 \langle (1 + k')^2 \rho / v \rangle_t + \frac{1}{96} \langle v (1 + 6k' + 11k'^2) \rho \rangle_t + \frac{2}{3} \langle v D_m d_f^2 k' \rho / D_s d_c^2 \rangle_t \right] \quad (8)$$

where the reduced velocity  $v$  is defined

$$v = u d_c / D_m \quad (9)$$

Eqns. 4–8 may also be written using reduced density,  $\rho_R = \rho / \rho_{cr}$ , where  $\rho_{cr}$  is the critical density of the mobile phase fluid.

### Resolution

Because of the significant effect of pressure drop on retention and efficiency in SFC, an exact expression for the general resolution equation is necessary. For a pair of Gaussian-shaped peaks, the resolution is

$$R_s = \frac{\Delta t_r}{2(\tau_1 + \tau_2)} \quad (10)$$

where  $t_r$  is retention time and  $\tau_1$  is the standard deviation of the first eluting peak expressed in units of time. In the usual derivation of the general resolution equation, an approximate equation is arrived at by assuming that for closely spaced peaks  $\tau_1 = \tau_2$ . This may not be an appropriate assumption in SFC, and the following equations are based on eqn. 10 as written. The apparent plate height is

$$\hat{H} = L \tau^2 / t_r^2 = L / \hat{N} \quad (11)$$

where  $L$  is column length and  $\hat{N}$  is the apparent number of theoretical plates. The retention time is [12,13]

$$t_r = t_0(1 + \hat{k}') \quad (12)$$

where  $t_0$  is the time required to elute an unretained species.

Combining eqns. 10–12 and rearranging yields

$$R_s = \frac{0.5(\hat{k}'_2 - \hat{k}'_1)\sqrt{L}}{(1 + \hat{k}'_1)\sqrt{\hat{H}_1} + (1 + \hat{k}'_2)\sqrt{\hat{H}_2}} \quad (13)$$

which is the desired equation expressing resolution in terms of apparent capacity factor and apparent plate height.

### DEVELOPMENT OF THE MODEL

#### Selection of a model system

Prediction of retention and efficiency from the equations presented above requires a knowledge of the effects of temperature and density on  $k'$ ,  $D_m$ ,  $D_s$ ,  $d_c$ , and  $d_f$ . Examination of the literature did not yield all of the desired experimental data for a single system. The expectation that the effect of density on  $k'$  is the most important factor in the generation of gradient-induced band spreading led to the selection of *n*-alkanes–CO<sub>2</sub>–polysiloxane as the solute–mobile phase–stationary phase system. The effect of temperature and density on retention for such systems has been treated theoretically [10], and extensive experimental data for a specific system have been recently obtained by Riester and Martire [19]. These data, for *n*-alkanes (C<sub>3</sub>–C<sub>22</sub>) on SB-octyl stationary phase (a methyloctylpolysiloxane, 50% methyl, 50% octyl substitution) over a wide range of temperature (320–380 K) and density (0.20–0.75 g/cm<sup>3</sup>), were subjected to an empirical fit to eqn. 1 to allow precise estimation of local and apparent capacity factors.

#### Effect of temperature and density on diffusion in the mobile phase

Solute diffusion coefficients were estimated from a modified form of the Wilke–Chang equation (see ref. 20) in which mobile phase density replaces viscosity

$$D_a \propto \frac{M_b^{0.5} T}{\rho_b V_a^{0.6}} \quad (14)$$

where the subscript *a* indicates the solute and *b* the solvent, and *D*, *M* and *V* represent the diffusion coefficient, molecular mass and molar volume, respectively. This relation is based on data from several studies [21–23] of solute diffusivity in dense gases, including supercritical CO<sub>2</sub>, which show that the product  $\rho D$  varies in a fairly well-defined fashion. Using naphthalene as a model solute, which is well-studied, the diffusivity of other non-polar solutes may be estimated.

*Effect of temperature and density on film thickness, column diameter and diffusion in the stationary phase*

The stationary phase in absorption SFC may absorb significant amounts of mobile phase, with concomitant changes in film thickness, effective column diameter, and the solute diffusion coefficient in the stationary phase. Changes in *k'* are reflected in the experimental data used in the model, and as such the effect of mobile phase sorption on retention will not be addressed directly. The impact on efficiency is treated here.

The swelling of the stationary phase due to uptake of mobile phase is represented by the swelling factor (*SF*)

$$SF = (V - V^0)/V^0 \quad (15)$$

where *V* and *V*<sup>0</sup> are the volumes of the swollen and unswollen film, respectively. Since the length of the film in an open tube is fixed, and if the thickness is small compared to the column radius, the volumetric change is proportional to the change in film thickness, and

$$SF = (d_f - d_f^0)/d_f^0 \quad (16)$$

where *d<sub>f</sub>* and *d<sub>f</sub>*<sup>0</sup> are the thickness of the swollen and unswollen film. The effective column diameter is

$$d_c = d_c^{00} - 2d_f \quad (17)$$

where *d<sub>c</sub>*<sup>00</sup> is the diameter of the uncoated tube. Thus both *d<sub>c</sub>* and *d<sub>f</sub>* can be easily estimated if the swelling factor is known.

Springston *et al.* [24] reported a swelling factor of  $1.0 \pm 0.6$  for SE-30 in the presence of supercritical CO<sub>2</sub> at 40°C and 88.8 atm ( $\rho_R = 1.05$ ). Swelling factors for SE-30 in the presence of butane were

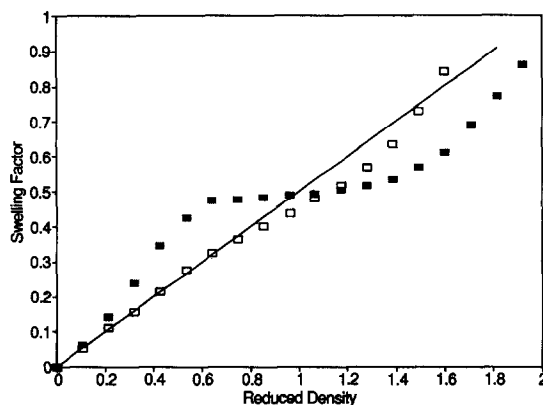


Fig. 1. Effect of CO<sub>2</sub> density on swelling of silicone rubber. ■ = 35°C; □ = 75°C; — = model. Experimental data taken from ref. 25.

greater and increased with increasing temperature. Shim and Johnston [25] measured the swelling of a silicone rubber film in the presence of CO<sub>2</sub> at pressures up to 300 bar and temperatures of 35°C and 75°C. Their experimental data are plotted as *SF* vs. reduced density in Fig. 1. The swelling factor increases almost linearly up to a reduced density of 0.5, levels off around a reduced density of 1, especially at the lower temperature, and then increases again with no indication of a maximum volume being reached. The swelling can be represented approximately by the simple equation

$$SF = 0.50\rho_R \quad (18)$$

While this is a much oversimplified expression, there is no reason to expect that the silicone rubber used by Shim and Johnston would behave identically to a polysiloxane stationary phase in an open capillary tube.

While knowledge of the swelling factor yields *d<sub>f</sub>* and *d<sub>c</sub>*, it yields no direct information about solute diffusion coefficients in the stationary phase. Rather, *D<sub>s</sub>* can be related to the mass fraction of mobile phase in the stationary phase, which bears no simple relationship to the swelling factor. Fujita [26] has shown that for a rubbery polymer impregnated with a low-molecular-mass diluent with diffusivity *D<sub>a</sub>*<sup>s</sup> in the swollen polymer, a plot of log *D<sub>a</sub>*<sup>s</sup> vs. mass fraction of diluent in the polymer,  $\phi$ , is approximately linear. Assuming that this relationship exists

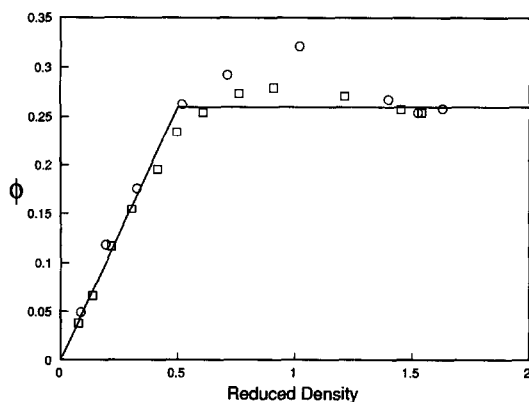


Fig. 2. Sorption of CO<sub>2</sub> by SE-30. ○ = 40°C; □ = 50°C; — = model. Experimental data taken from ref. 28.

across the entire range of concentrations, we have the equation

$$\log D_a^s = (1 - \phi) \log D_a^{s0} + \phi \log D_a^m \quad (19)$$

where  $D_a^{s0}$  and  $D_a^m$  are the diffusion coefficients of the diluent in the pure polymer (stationary phase) and pure diluent (mobile phase), respectively. We will assume that the equation also applies to *solute* diffusion coefficients in the stationary and mobile phases, where  $D_a^s$  and  $D_a^{s0}$  are equivalent to  $D_s$  and  $D_s^0$ , the solute diffusion coefficients in the swollen and unswollen stationary phase, respectively.

In order to utilize eqn. 19, we must evaluate  $\phi$ ,  $D_a^{s0}$  and  $D_a^m$ . The value of  $D_a^{s0}$  is estimated from the equation developed by Kong and Hawkes [27] for diffusion of normal alkanes in polysiloxane stationary phases. The estimations of  $\phi$  and  $D_a^m$  are discussed in the following paragraphs.

Mass sorption isotherms for CO<sub>2</sub> in polysiloxanes have been reported by several workers [28–30]. Of these only the report by Strubinger *et al.* [28] provides data for the CO<sub>2</sub>–SE-30 system at temperatures and pressures of interest in SFC. Their data for 40 and 50°C at pressures up to 160 bar are presented in Fig. 2 in terms of reduced density as the independent variable. Both sets of data exhibit a maximum around the critical density, a phenomenon also observed by Yonker and Smith [29] for the CO<sub>2</sub>–SE-54 system. At high densities, all curves (including the isotherm for 35°C, not shown) converge to a value of  $\phi = 0.26$ . These phenomena, especially the occurrence of maxima, are not well understood. Yonker

and Smith have suggested that surface adsorption may play a significant role in these systems. One possible explanation is that both absorption and adsorption occur, where the sorption of CO<sub>2</sub> occurs largely by *absorption*, as represented by the solid line in Fig. 2, and the excess sorption is due to *adsorption*, leading to the maxima observed around the critical density. Whatever the case, the situation poses some uncertainty with regard to the effect of  $\phi$  on  $D_s$ . For the purpose of the application of eqn. 19 to the model, then, let us choose the simple case represented by the solid line in Fig. 2, where

$$\phi = 2\rho_R \phi_{\max} \quad (\rho_R \leq 0.5) \quad (20a)$$

$$\phi = \phi_{\max} \quad (\rho_R > 0.5) \quad (20b)$$

For the CO<sub>2</sub>–polysiloxane system, we set  $\phi_{\max} = 0.26$  for all temperatures.

Next we examine the value of  $D_a^m$  in eqn. 19.  $D_a^m$  in this case represents the solute diffusion coefficient in the mobile phase at a density corresponding to the specific volume of the mobile phase component in the swollen stationary phase. Strubinger *et al.* [28] have shown that the specific volume of CO<sub>2</sub> in SE-30,  $\hat{V}_1^L$ , is about 1.1 cm<sup>3</sup>/g at low values of pressure and  $\phi$ , but that it increases significantly at increased pressure. This is a result of the fact that, while the amount of CO<sub>2</sub> sorbed reaches a maximum at high pressures (Fig. 2), the swelling factor increases continuously as pressure is increased (Fig. 1). In our model, the value of  $\hat{V}_1^L$  can be calculated from the relation

$$\hat{V}_1^L = \frac{SF(1 - \phi)}{\phi \rho_s^0} \quad (21)$$

where  $\rho_s^0$  is the density of the pure stationary phase [27]. The value of  $D_a^m$  used in eqn. 19 is then calculated from the modified Wilke–Chang equation (as  $D_a$  in eqn. 14) at a CO<sub>2</sub> reduced density of

$$\rho_R = \frac{1}{\hat{V}_1^L \rho_{cr}} \quad (22)$$

The critical density of CO<sub>2</sub>,  $\rho_{cr}$ , is taken as 0.468 g/cm<sup>3</sup>.

The net effect of  $SF$  and  $\phi$  on  $D_s$  is shown in Fig. 3 for C<sub>24</sub> at 40°C. The model predicts that  $D_s$  increases more than ten-fold as CO<sub>2</sub> density is increased from  $\rho_R = 0$  to  $\rho_R = 0.5$ . While  $\phi$  is assumed to be constant above  $\rho_R = 0.5$ ,  $D_s$  continues to increase

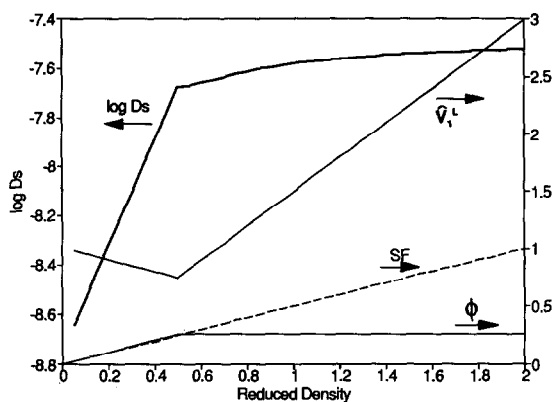


Fig. 3. Effect of stationary phase swelling on diffusivity. Predictions of the model for  $n\text{-C}_{24}\text{H}_{50}$  at  $40^\circ\text{C}$ .

slightly due to continued swelling of the stationary phase. The value of  $\hat{V}_1^L$  decreases from 1.0 to 0.8 at  $\rho_R < 0.5$ , in reasonably good agreement with the value of 1.1 predicted by Strubinger *et al.* [28], and then rises continuously as density increases due to the combined effects of a continuously increasing  $SF$  while  $\phi$  remains constant. The negative slope at low densities is an artifact of the treatment, arising from a somewhat inexact description of the swelling behavior.

There is a substantial difference between this system and those treated by Fujita. In the latter systems the penetrants were condensed phases such as benzene at room temperature, for which the partial molar volume of the penetrant inside the polymer is assumed to be equal to the bulk liquid value. For the  $\text{CO}_2$ -polysiloxane system, the specific volume of  $\text{CO}_2$  rises dramatically for  $\rho_R > 0.5$ . The treatment here accounts for this by adjusting the value of  $D_b$  in eqn. 19, so that even though  $\phi$  is assumed constant at  $\rho_R > 0.5$ ,  $\log D_s$  continues to increase with  $\rho_R$  at a moderate rate. However, the large increase in  $\hat{V}_1^L$  at  $\rho_R > 0.5$  suggests a loosening of the cross-linked polymer network, which would further enhance diffusion in the swollen polymer. Even though the present treatment predicts substantial increases in  $D_s$  at low mobile phase densities, it may in fact severely underestimate the values of  $D_s$  at higher densities.

#### COMPUTATIONAL APPROACH

The calculation of temporal and spatial average

quantities has been described elsewhere [12,13]. Computations were performed on an IBM-compatible personal computer with an Intel 80386 microprocessor and 80387 math coprocessor, using an extension of a program written in Microsoft QuickBASIC for modelling retention and efficiency of packed columns [15].

A Van Deemter plot is typically prepared by measuring apparent plate height as a function of velocity while maintaining other conditions constant so that, among other things,  $\hat{k}'$  does not vary with flow-rate. This is not possible in SFC because  $k'$  varies along the column. However, at low pressure drops  $\hat{k}'$  is approximately a quadratic function of  $\langle \rho \rangle_t$  [12]

$$\ln \hat{k}' = \ln \langle k' \rangle_t \approx \ln k'^0 - a \langle \rho_R \rangle_t + b \langle \rho_R \rangle_t^2 \quad (23)$$

In order to obtain results at constant  $\hat{k}'$ , at least in the low velocity, low pressure-drop region, all measurements should be done at the same temporal average density. Results obtained in this fashion may be compared with results obtained for non-compressible fluids.

The basic computational approach therefore mimics a series of isothermal SFC experiments for the elution of a pair of  $n$ -alkanes in which the mass flow-rate, which is held constant for a given experiment, is incremented while maintaining the same temporal average mobile phase density for all experiments. This is done for  $\langle \rho_R \rangle_t = 1.0, 1.2, 1.4, 1.6$  and  $1.8$ , at temperatures of  $40, 80$  and  $120^\circ\text{C}$ . The result is a set of Van Deemter plots, each corresponding to a single temperature and temporal average density. All calculations for this study were done for an open-tubular column of  $30 \text{ m} \times 50 \mu\text{m}$  I.D. with a  $0.25\text{-}\mu\text{m}$  thick film of stationary phase. For successive experiments, the mass flow-rate is increased by simultaneously increasing the inlet pressure and decreasing the outlet pressure so that the selected temporal average density is maintained. This approach yields Van Deemter plots which, at low flow-rates, are similar to those traditionally produced for liquid or gas chromatography.

#### PREDICTIONS OF THE MODEL

##### *Mobile phase density, velocity and pressure*

The inlet and outlet pressures required to achieve

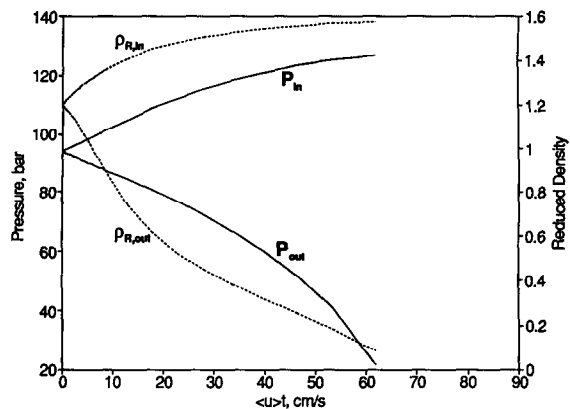


Fig. 4. Pressure and reduced density at column inlet and outlet for CO<sub>2</sub> at 40°C and  $\langle \rho_R \rangle_t = 1.2$ . Column: open-tubular, 30 m × 50 μm I.D. × 0.25 μm film, SB-octyl stationary phase. Dashed lines are plotted against right axis.

desired flow-rates while maintaining the same temporal average density are shown in Fig. 4 for  $\langle \rho_R \rangle_t = 1.2$  at 40°C. Values of the corresponding inlet and outlet reduced densities (dashed curves) are plotted against the right axis. In general, the curves for low temperature (40°C) and low density showed a non-linearity similar to that in Fig. 4, whereas at higher temperatures and densities the curves were more linear. Fig. 4 demonstrates that simply maintaining the same average column pressure while adjusting the flow-rate will not in general result in maintaining the same temporal average density.

*Effect of temperature, density and solute on efficiency*

Fig. 5 shows a family of curves for apparent plate

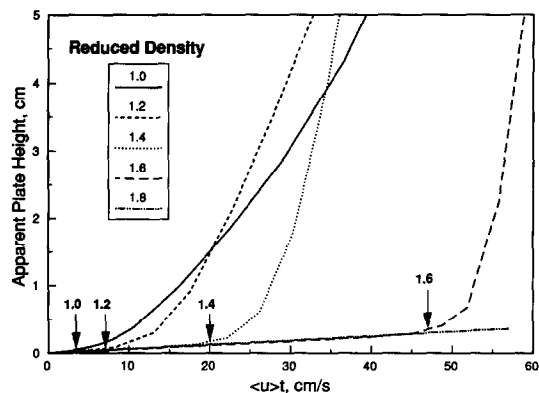


Fig. 5. Apparent plate height vs. temporal average linear velocity at various mobile phase densities for C<sub>16</sub> at 40°C.

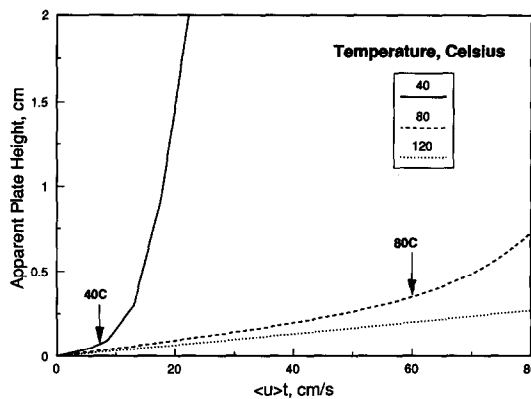


Fig. 6. Apparent plate height vs. temporal average linear velocity at different temperatures for C<sub>16</sub> at  $\langle \rho_R \rangle_t = 1.2$ .

height vs. temporal average linear velocity,  $\langle u \rangle_t$ , for C<sub>16</sub> at 40°C and various mobile phase densities. The curves at lower  $\langle \rho_R \rangle_t$  show significant loss of efficiency as the linear velocity is increased. These curves are similar to those reported elsewhere [1,15, 17]. Extremely large plate height values are observed at high velocities, especially at low mobile phase densities. The arrows identify the onset of GIBS (see below).

The effect of temperature on  $\hat{H}$  for elution of C<sub>16</sub> at  $\langle \rho_R \rangle_t = 1.2$  is shown in Fig. 6. At elevated temperatures it should be possible to operate at much higher velocities before GIBS becomes a significant problem. This is due to the decreased compressibility of CO<sub>2</sub> at the higher temperatures.

The effect of solute on  $\hat{H}$  at 40°C and  $\langle \rho_R \rangle_t =$

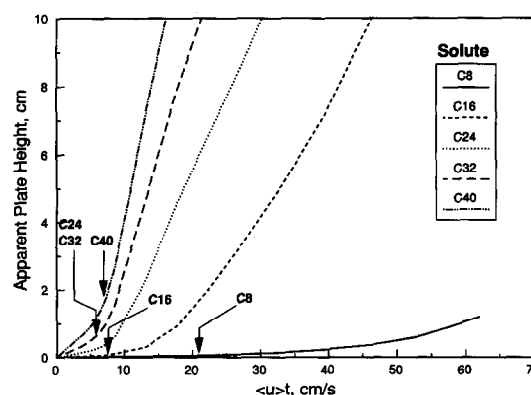


Fig. 7. Apparent plate height vs. temporal average linear velocity for five n-alkanes at 40°C and  $\langle \rho_R \rangle_t = 1.2$ .

1.2 is shown in Fig. 7. Severe losses in efficiency occur for the long-chain alkanes at even moderate velocities. These systems are examined in greater detail below.

#### Contribution of gradient-induced band spreading to apparent plate height

The loss of efficiency at higher velocities in Figs. 5-7 is attributable to the presence of solute velocity gradients [15]. These gradients arise from the expansion of the mobile phase and the corresponding increases in mobile phase velocity and solute capacity factor as the solute band travels along the column. An estimate of the relative contribution of this effect to the overall dispersion can be obtained by examination of the following terms:

(i) the reduced plate height assuming density is constant at  $\langle \rho_R \rangle_t$  with no swelling

$$h_{\text{set}} = \frac{2}{v_{\text{set}}} + \frac{v_{\text{set}}(1 + 6k'_{\text{set}} + 11k'^2_{\text{set}})}{96(1 + k'_{\text{set}})^2} + \frac{2v_{\text{set}}D_{\text{mset}}(d_f^0)^2 k'_{\text{set}}}{3D_s^0(d_c^0)^2(1 + k'_{\text{set}})^2} \quad (24)$$

(ii) the reduced plate height assuming constant conditions at  $k' = \langle k' \rangle_t$  with no swelling

$$h_{\text{est}} = \frac{2}{v_{\text{set}}} + \frac{v_{\text{set}}(1 + 6\langle k' \rangle_t + 11\langle k' \rangle_t^2)}{96(1 + \langle k' \rangle_t)^2} + \frac{2v_{\text{set}}D_{\text{mset}}(d_f^0)^2 \langle k' \rangle_t}{3D_s^0(d_c^0)^2(1 + \langle k' \rangle_t)^2} \quad (25)$$

(iii) the reduced plate height assuming mobile phase GIBS with no swelling

$$h_{\text{set2}} = \frac{1}{\langle 1 + k' \rangle_t^2 \langle \rho_R \rangle_t} \left[ \frac{2}{v_{\text{set2}}} \langle (1 + k')^2 \rho_R \rangle_t + \frac{v_{\text{set2}}}{96} \langle (1 + 6k' + 11k'^2) \rho_R \rangle_t + \frac{2v_{\text{set2}}(d_f^0)^2}{3D_s^0(d_c^0)^2} \langle D_m \rho_R k' \rangle_t \right] \quad (26)$$

The subscript "set" sets the corresponding mobile phase parameter to its value at a reduced density equal to  $\langle \rho_R \rangle_t$ , and the superscript "0" sets the stationary phase parameter to its value in the absence of swelling. The subscript "set2" indicates that the mobile phase parameters are allowed to vary, but the stationary phase parameters are con-

stant with no swelling. Both  $h_{\text{set}}$  and  $h_{\text{est}}$  are estimates of the reduced plate height which would be obtained in the absence of GIBS and stationary phase swelling, *i.e.*, all column parameters are constant. These two terms differ only in that  $h_{\text{set}}$  employs  $k'_{\text{set}}$ , whereas  $h_{\text{est}}$  employs  $\langle k' \rangle_t$  as the value of the capacity factor.  $h_{\text{set2}}$  provides an estimate of the apparent plate height which would be observed due to mobile phase GIBS only, with no swelling of the stationary phase.

The dependence of  $\hat{h}$ ,  $h_{\text{est}}$ ,  $h_{\text{set}}$ ,  $h_{\text{set2}}$  and  $\langle k' \rangle_t$  on reduced velocity is shown in Fig. 8 for the elution of  $C_{16}$  at 40°C and  $\langle \rho_R \rangle_t = 1.2$ . [Note. To facilitate comparison with other figures, the point at which  $\langle u \rangle_t = 5 \text{ cm/s}$  is indicated in Figs. 8-10. The relationship between  $\langle u \rangle_t$  and  $\langle v \rangle_t$  may be taken as approximately linear.] At  $\langle v \rangle_t = 2900$ ,  $\hat{h}$  reaches a value of 5000, about 50 times greater than  $h_{\text{set}}$ , and about 18 times greater than  $h_{\text{est}}$ . In contrast,  $h_{\text{set2}}$  is essentially identical to  $\hat{h}$  over the entire range of velocities, indicating that the increased band spreading (relative to  $h_{\text{set}}$  or  $h_{\text{est}}$ ) is due almost entirely to mobile phase GIBS. For this system, then, GIBS is by far the major contribution to dispersion at high velocities for this system, and essentially all of the GIBS is due to changes in the mobile phase.

An estimate of the onset of GIBS is given by the ratio of  $h_{\text{set2}}$  over  $h_{\text{set}}$  or by  $h_{\text{set2}}$  over  $h_{\text{est}}$ . The point at which the ratio  $h_{\text{set2}}/h_{\text{est}}$  exceeds 1.1 is marked by an arrow on each of the curves in Figs. 5-7. The onset of GIBS occurs at higher velocities as  $\langle \rho_R \rangle_t$

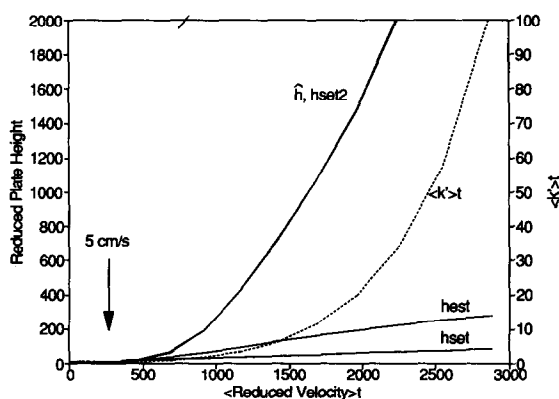


Fig. 8. Estimates of reduced plate height for elution of  $C_{16}$  at 40°C and  $\langle \rho_R \rangle_t = 1.2$ . Dashed line is plotted against right axis.

is increased (Fig. 5). Higher operating temperatures also increase the velocity for onset of GIBS (Fig. 6). Fig. 7 shows that GIBS occurs at roughly the same velocity for  $C_{16}$ – $C_{40}$  at  $40^\circ\text{C}$  and  $\langle\rho_R\rangle_t = 1.2$ , but at a significantly higher velocity for  $C_8$ .

#### Contributions from the individual plate height terms

Under conditions of laminar flow, the apparent reduced plate height in open-tubular chromatography is the sum of three terms,

$$\hat{h} = \hat{h}_l + \hat{h}_m + \hat{h}_s \quad (27)$$

where the subscripts l, m, and s refer, respectively, to longitudinal diffusion in the mobile phase, radial mixing in the mobile phase, and resistance to mass transfer in the stationary phase. A plot of the apparent reduced plate height vs.  $\langle v \rangle_t$  for  $C_{16}$  at  $40^\circ$  and  $\langle\rho_R\rangle_t = 1.2$  appears in Fig. 9, along with  $h_{set}$  and  $\langle k' \rangle_t$ . At high reduced velocities, where  $\hat{h} \gg h_{set}$ , the total dispersion is due almost entirely to the mobile phase mixing term  $\hat{h}_m$ ; the  $\hat{h}_l$  and  $\hat{h}_s$  terms are insignificant and are not visible in the figure. This is true also at the lower velocities, and in general for  $C_{16}$  at other temperatures and densities. A much different result is obtained for  $C_{32}$  at  $40^\circ\text{C}$  and  $\langle\rho_R\rangle_t = 1.4$  (Fig. 10). At reduced velocities below 1500,  $\hat{h}_s$  is the dominant term. At higher velocities  $\hat{h}_m$  becomes the dominant term because of the onset of GIBS, and  $\hat{h}_s$  decreases because of the increase in capacity factor.

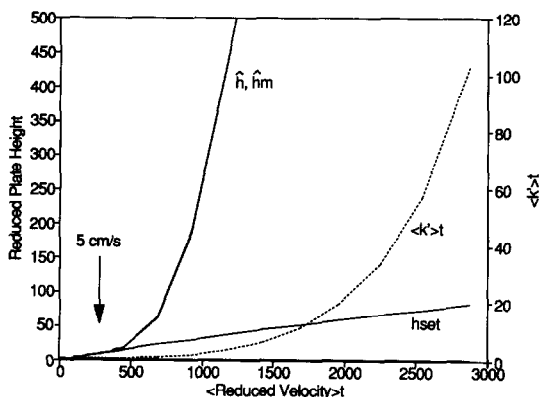


Fig. 9. Contributions of individual plate height terms to apparent reduced plate height for  $C_{16}$  at  $40^\circ\text{C}$  and  $\langle\rho_R\rangle_t = 1.2$ . The  $\hat{h}_l$  and  $\hat{h}_s$  terms are too small to be seen. The  $h_{set}$  curve shows expected efficiency in absence of GIBS and swelling. Dashed line is plotted against right axis.

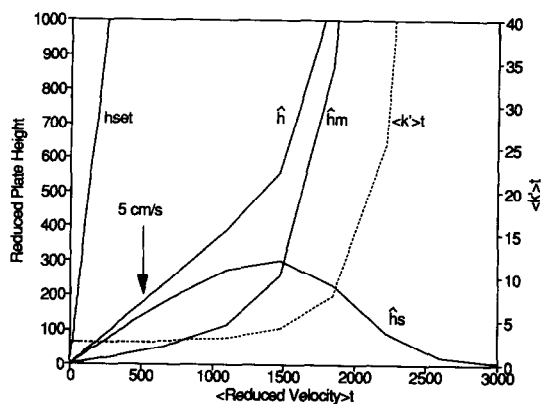


Fig. 10. Contributions of individual plate height terms to apparent reduced plate height for  $C_{32}$  at  $40^\circ\text{C}$  and  $\langle\rho_R\rangle_t = 1.4$ . Dashed line is plotted against right axis.

#### Effects of temperature and swelling on the stationary phase term

Note that the  $h_{set}$  term for  $C_{32}$  in Fig. 10 is much larger than the apparent plate height. This large value of  $h_{set}$  is due to the stationary phase term, resulting from a very small predicted value of  $D_s^0$  for  $C_{32}$  at this temperature [27]. The true magnitude of the stationary phase term at low temperatures is somewhat questionable because the value of  $D_s^0$  used represents an extrapolation of the experimental data obtained by Kong and Hawkes. Normally in gas chromatography the stationary phase term for  $C_{32}$  would be much smaller due to the higher temperatures used and better diffusivity in the stationary phase; at lower temperatures poor diffusion in that stationary phase would be a problem even if reasonable retention times could be obtained. These predictions of the model suggest that the sorption of mobile phase by stationary phase, and the attendant swelling which results, may be largely responsible for the achievement of acceptable efficiency in the separation of high-molecular-mass solutes at low temperatures by SFC.

#### Retention time and resolution

Retention time and resolution are two parameters which are of great practical importance in chromatography. Other parameters held constant, a decrease in retention time produced by an increase in flow-rate is generally obtained at the expense of decreased resolution. The extremely large values of

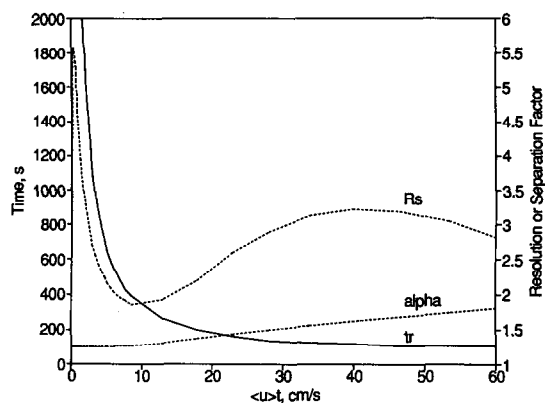


Fig. 11. Retention time for  $C_9$  and its resolution from  $C_8$  at  $40^\circ\text{C}$  and  $\langle\rho_R\rangle_t = 1.2$ . Symbols:  $t_r$  = retention time;  $\alpha$  = separation factor;  $R_s$  = resolution. Dashed lines are plotted against right axis.

apparent plate height due to GIBS which are generated at high velocities in SFC strongly suggest that one should avoid large pressure drops in SFC. However, the data presented in Fig. 11 show that it should be possible to simultaneously reduce the retention time and improve resolution by increasing the flow-rate. Fig. 11 shows the predicted retention time for  $C_9$  and its resolution from  $C_8$  for their elution at  $40^\circ\text{C}$  and  $\langle\rho_R\rangle_t = 1.2$ . The resolution was calculated using eqn. 13. Two maxima appear in the  $R_s$  vs.  $\langle u \rangle_t$  curve; one as expected at very low velocity ( $R_s = 5.5$  at  $\langle u \rangle_t = 0.35$  cm/s,  $t_r = 2.7$  h, barely visible near the origin), and the other at a very

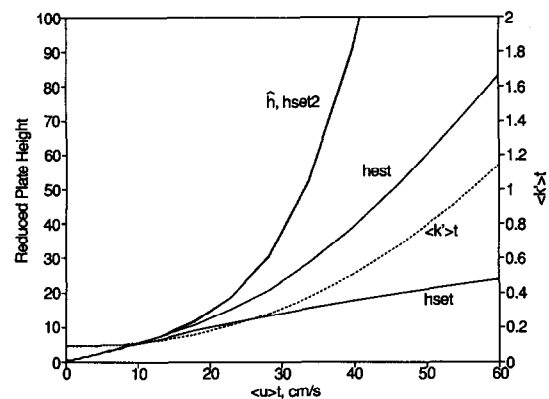


Fig. 12. Estimates of reduced plate height for elution of  $C_9$  at  $40^\circ\text{C}$  and  $\langle\rho_R\rangle_t = 1.2$ . Dashed line is plotted against right axis.

high velocity ( $R_s = 3.2$  at  $\langle u \rangle_t = 40$  cm/s,  $t_r = 110$  s). The latter resolution is also obtained at  $\langle u \rangle_t = 2.0$  cm/s with  $t_r = 1700$  s, or about 28 min. The second resolution maximum occurs under conditions where GIBS is the dominant source of dispersion and the apparent reduced plate height is greater than 100 (Fig. 12). This unusual behavior is produced by the simulated experimental conditions (see Computational approach section), and appears to be due to an increase in the separation factor,  $\alpha$ , at high velocities, also shown in Fig. 11. The separation factor is defined [13]

$$\alpha = \hat{k}'_2 / \hat{k}'_1; \quad \hat{k}'_2 > \hat{k}'_1 \quad (28)$$

While  $\hat{k}'$  for  $C_9$  increases at high flow-rates, it increases somewhat less rapidly for  $C_8$ , leading to the increased separation factor and the improved resolution at high flow-rates. As the velocity increases beyond 40 cm/s,  $\alpha$  continues to increase, but resolution decreases due to the overwhelming effect of GIBS. Resolution curves with two maxima were observed for other solutes and at other conditions in this study, but in most cases the rapid increase in GIBS prevented significant improvements in resolution at high velocities. This example does however point out the possibility of performing very rapid separations by using large pressure drops and flow-rates in SFC.

## CONCLUSIONS

This model takes into account recently developed theories for retention and efficiency, as well as the observed effects of temperature and mobile phase density on system parameters, to produce realistic predictions of retention, efficiency and resolution in open-tubular SFC. The excessive band spreading often observed at high pressure drops, or GIBS, is due primarily to mobile phase processes. The maximum pressure drop and linear velocity which can be used before GIBS becomes significant depends on a combination of temperature, temporal average density and solute. In general, GIBS may be largely avoided by working at densities and temperatures well above the critical values. Sorption of mobile phase by the stationary phase appears to be critical to the achievement of acceptable efficiency in the separation of high-molecular-mass solutes at the

low temperatures commonly used in SFC, due to the improved solute diffusivity in the swollen stationary phase. However, a better understanding of the effect of swelling on diffusivity is required to accurately predict the magnitude of the effect. Finally, the effect of density drop on separation factor has the potential to make possible very fast separations by SFC.

#### ACKNOWLEDGEMENTS

The author thanks Rebecca Riester of Georgetown University for supplying experimental retention data, and appreciates the useful discussions with Daniel Martire of Georgetown University and Tim Lodge of the University of Minnesota, Twin Cities. Support for this work was provided through a Grant-in-Aid of Research from the Graduate School of the University of Minnesota. The basic theoretical work was initiated while the author was on sabbatical leave at Georgetown University with support from the Bush Sabbatical Program of the University of Minnesota, and the National Science Foundation grant number CHE-8902735.

#### REFERENCES

- 1 P. A. Mourier, M. H. Caude and R. H. Rosset, *Chromatographia*, 23 (1987) 21.
- 2 P. J. Schoenmakers and L. G. M. Uunk, *Chromatographia*, 24 (1987) 51.
- 3 T. A. Berger and J. F. Deye, *Chromatographia*, 30 (1990) 57.
- 4 H. Engelhardt, A. Gross, R. Mertens and M. Petersen, *J. Chromatogr.*, 477 (1989) 169.
- 5 D. R. Gere, R. Board and D. McManigill, *Anal. Chem.*, 54 (1982) 736.
- 6 T. A. Dean and C. F. Poole, *J. Chromatogr.*, 468 (1989) 127.
- 7 B. P. Semonian and L. B. Rogers, *J. Chromatogr. Sci.*, 16 (1978) 49.
- 8 P. A. Peaden and M. L. Lee, *J. Chromatogr.*, 259 (1983) 1.
- 9 S. M. Fields, R. C. Kong, J. C. Fjelstad, M. L. Lee and P. A. Peaden, *J. High Resolut. Chromatogr. Chromatogr. Commun.*, 7 (1984) 312.
- 10 D. E. Martire and R. E. Boehm, *J. Phys. Chem.*, 91 (1987) 2433.
- 11 D. E. Martire, *J. Liq. Chromatogr.*, 10 (1987) 1569.
- 12 D. E. Martire, *J. Chromatogr.*, 461 (1989) 165.
- 13 D. E. Martire, R. L. Riester, T. J. Bruno, A. Hussam and D. P. Poe, *J. Chromatogr.*, 545 (1991) 135.
- 14 X. Zhang, D. E. Martire and R. G. Christiansen, Georgetown University and National Institute for Science and Technology, Washington, DC, 1990, unpublished results.
- 15 D. P. Poe and D. E. Martire, *J. Chromatogr.*, 517 (1990) 3.
- 16 J. C. Giddings, *Dynamics of Chromatography*, Marcel Dekker, New York, 1965, pp. 79-82.
- 17 H.-G. Janssen, P. J. Schoenmakers, H. M. J. Sniijders, J. A. Rijks and C. A. Cramers, *J. High Resolut. Chromatogr.*, 14 (1991) 438.
- 18 L. M. Blumberg and T. A. Berger, *J. Chromatogr.*, 596 (1992) 1.
- 19 R. Riester and D. E. Martire, Georgetown University, Washington, DC, 1991, unpublished results.
- 20 R. C. Reid, J. M. Prausnitz and B. E. Poling, *The Properties of Liquids and Gases*, McGraw-Hill, New York, 4th ed., 1987.
- 21 I. Swaid and G. M. Schneider, *Ber. Bunsenges. Phys. Chem.*, 83 (1979) 969.
- 22 R. Feist and G. M. Schneider, *Sep. Sci. Technol.*, 17 (1982) 261.
- 23 Z. Balenovic, M. N. Myers and J. C. Giddings, *J. Chem. Phys.*, 52 (1970) 915.
- 24 S. R. Springston, P. David, J. Steger and M. Novotny, *Anal. Chem.*, 58 (1986) 997.
- 25 J.-J. Shim and K. P. Johnston, *AIChE J.*, 35 (1989) 1097.
- 26 H. Fujita, *Fortschr. Hochpolym.-Forsch.*, 3 (1961) 1.
- 27 J. M. Kong and S. J. Hawkes, *J. Chromatogr. Sci.*, 14 (1976) 279.
- 28 J. R. Strubinger, H. Song and J. F. Parcher, *Anal. Chem.*, 63 (1991) 98.
- 29 C. R. Yonker and R. D. Smith, *J. Chromatogr.*, 505 (1990) 139.
- 30 G. K. Fleming and W. J. Koros, *Macromolecules*, 19 (1986) 2285.